UNIVERSITY OF GOTHENBURG

DEPARTMENT OF BIOLOGICAL AND ENVIRONMENTAL SCIENCES

GENETIC CONTROL OF STOMATAL PATTERN IN COMMON BEAN

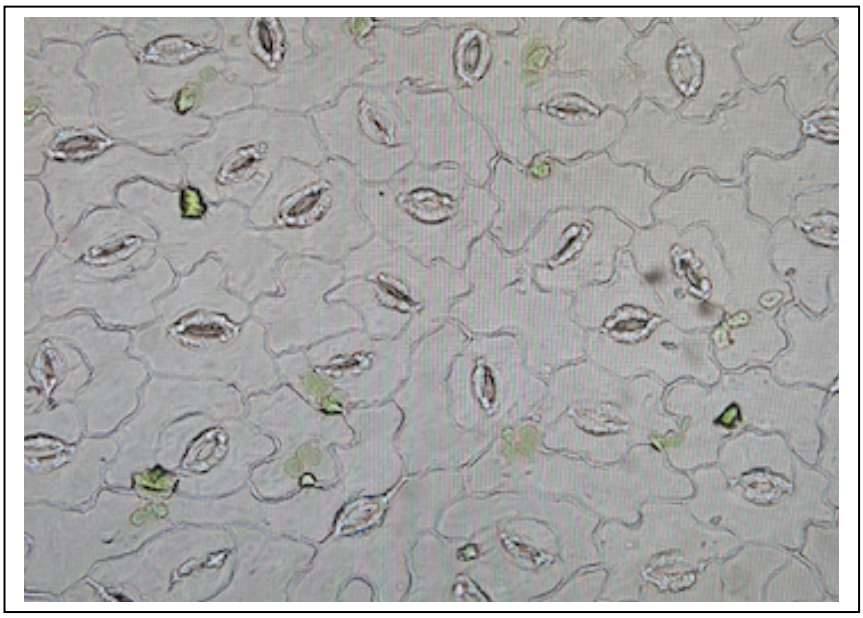

Wilma Berg

Degree project for Bachelor of Science with a major in Biology
BIO603, Biology: Bachelor´s degree project 30 credits
First cycle
Semester/year: Spring 2026
Supervisor: Mats Andersson
Examiner: Cornelia Spetea Wiklund

Index

1. Introduction **2**

1.1 Common bean *2*

1.2 Stomata and the effect of density and size on photosynthesis and water economy *2*

1.3 Genetic mapping *3*

2. Aim **4**

3. Material and method **4**

3.1 Plant material and growth conditions *4*

3.2 Investigation of stomatal traits *4*

3.3 Data analysis *5*

4. Results **6**

4.1 Genetic variation in common bean parental lines *6*

4.2 Genetic mapping of common bean MAGIC lines *7*

5. Discussion **9**

6. Conclusion **11**

7. References **12**

Abstract

Common bean (*Phaseolus vulgaris)* is an important legume crop in many low-income countries and a major source of protein and micronutrients. In recent years, increasing temperatures and drought stress have decreased global bean production, with approximately 60% of current cultivations experiencing yield loss. The intake of carbon dioxide is done through stomata, microscopic pores on the leaf epidermis. However, stomata also serve as the primary pathway for water vapor loss through transpiration. Stomatal conductance is tightly regulated by stomatal traits, and identifying traits associated with improved drought tolerance and water use could support selective breeding of more resilient bean cultivars. To investigate a genetic basis of stomatal traits a multiparent advanced generation intercross (MAGIC) population of common bean was used. The population consisted of 500 inbred MAGIC lines containing recombined founder genotypes of eight parent lines with the aim to identify lines with enhanced drought tolerance. In this study microscopy was conducted on the eight parent lines and 200 MAGIC lines. Stomatal area, length and density were measured, and the theoretical maximal stomatal conductance was calculated for each line. A quantitative trait locus (QTL) analysis identified a significant peak for stomatal area on chromosome 1. No significant QTL-peaks were identified for the remaining stomatal traits. Within the QTL interval, 95 candidate genes were identified, including leucine-rich repeats, receptor-like kinases as well as other genes potentially involved in the regulation of stomatal area. Furthermore, a clear negative correlation between stomatal density and area was identified in both parent and MAGIC populations, with the MAGIC population displaying a broader variation. These findings improve our understanding of the genetic and phenotypic regulation of stomatal traits, and the detected QTL-region provides a foundation for future research of stomatal regulation and adaptation to drought in common bean.

Key words: common bean, stomata, MAGIC population, QTL, genetic mapping

1. Introduction

1.1 Common bean

Common bean (*Phaseolus vulgaris)* is a valuable food resource mainly grown in Africa and America. Due to their high nutrient content and inexpensive cultivation, it is a valuable resource of protein in developing countries (Castro-Guerrero et al. 2016). Bean cultivations worldwide are negatively affected by drought, an increasing issue driven by climate change specifically in developing countries. Even a moderate amount of drought stress has been shown to decrease biomass, seed yield and weight (Pathania et al. 2014). Around 60% of the worlds common bean production suffers because of drought and cultivations in southeastern Africa are estimated to have insufficient growth conditions for common bean by the year 2050 (Hummel et al. 2018; Polania et al. 2016). Varieties of common bean are currently being developed to withstand climate change to maintain future production. (Diaz. et al. 2020)

Subspecies of common bean originate from two primary gene pools, the Andean pool from South America and the Mesoamerican pool from Central America and Mexico. Races within the species differ in genetically controlled characteristics such as seed size, seed color and stomatal attributes due to variation and local adaptions in allelic frequencies at specific loci (Pathania, et.al. 2014). Agronomic characteristics influence yield, water requirements and tolerance to environmental stress or diseases, making them important targets in crop breeding programs to improve performance in disadvantageous conditions such as drought (Yoosefzadeh-Najafabadi et al. 2023; Samantara et al. 2021). The Andean and Mesoamerican gene pools belong to the primary gene pool and can generally interbreed to produce fertile offspring, although some incompatibility can occur (Pathania et al. 2014). In addition, common bean also exhibits interspecific relationships through secondary, tertiary, and quaternary gene pools including related species that can cross hybridize under specific conditions, however the hybrid offspring is generally sterile (Pathania et al. 2014). Altogether the genetic variation within and between common bean gene pools provide an important foundation when investigating genetic control of stomatal traits in the role of adapting to environmental stress conditions.

1.2 Stomata and the effect of density and size on photosynthesis and water economy

The stomata are microscopic pores responsible for a plant's gas exchange with the environment, particularly the uptake of carbon dioxide used for photosynthesis (Hetherington & Woodward. 2003). They also play a role in the plants water economy, as water vapor exit through the same pathway. Stomata are distributed over the epidermis of plant leaves with at least one epidermal cell separating each stoma for an efficient function. The stomata itself consist of a pore surrounded by two guard cells that are either kidney- or dumbbell shaped depending on the plant species. Normally the length of stomata ranges from 10-80 μm (Hetherington & Woodward. 2003). The plant can control the guard cells through alteration in turgor pressure resulting in closed or open stomata pores and through this, control gas exchange with the atmosphere. Guard cells regulate stomatal aperture in response to environmental factors such as light, temperature, water availability and CO_2 concentration in the air (Harrison et al. 2019). During drought, guard cells are signaled to decrease their turgor pressure, causing the stomatal aperture to decrease and reduce water loss. However, this occurs at the expense of CO_2 uptake for photosynthesis (Bertolino et al. 2019). The intrinsic water use efficiency (iWUE) of plants is the balance between a plants carbon fixation in photosynthesis and transpiration that need to be maintained in a functioning plant. It is obtained either by control of stomatal aperture, referring to adjustments in stomatal pore size or by regulation

of stomatal density during plant development. Arguably the outcome of reducing stomatal density is a lowered photosynthesis and stomatal conductance, however, studies has identified an increase in drought tolerance without decreased photosynthesis (Harrison. 2019).

Plant photosynthesis and water economy are controlled by morphological traits of the stomata such as size, shape, and density that can be regulated during leaf formation. There is not a single optimal relationship between maximal pore area and stomatal density in nature. Although most plants can achieve a maximal potential in response to environmental factor in their environment and only acquire maximum gas exchange capacity during extreme environmental changes. It has been observed that a higher stomata density results in stomata of smaller size, and on the contrary larger stomata correspond to a lower density (Haworth et al. 2023). The size of stomata affects how quickly the guard cells surrounding the stomata respond to environmental changes. Smaller stomata are generally faster in response compared to larger stomata due to the requirement of smaller changes in volume. The size of stomata is furthermore related to genome size of the plant. A larger genome corresponds to a lower stomatal density and larger individual size (Harrison. 2019). Genetical differences between stomatal traits is the main factor influencing photosynthesis and water-use efficiency. These adaptions enable the plant to balance carbon uptake and water conservation in different environmental conditions.

1.3 Genetic mapping

Genetic mapping is the process of locating physical positions in the genome through genetic markers. By identifying regions of interest on the chromosome it is possible to dissect quantitative traits connected to important attributes in areas such as agriculture (Seidl. et al. 2016). There are two kinds of mapping, the genetic or linkage maps and physical mapping. Genetic mapping is based on mating experiments and uncover information on gene transfer, recombinants frequency and species relationships (Clark & Pazdernik. 2016). Linkage maps are based on the probability that two traits segregate together, and the closer two genes are on the chromosome, the lower the chance is of them segregating after recombination. Physical mapping on the other hand can identify the physical distance between markers on the chromosome in base pairs, while genetic mapping identifies the distance in centimorgans. (Clark & Pazdernik. 2016). Both variations of mapping identify quantitative traits loci (QTLs), the region itself associated with the quantitative traits. The key with linkage analysis is to figure out where on the genome this variation in gene expression exist. For a long time, bi-parental populations have been used as genetic markers to identify QTLs. However, due to the low allele frequencies in a two parental population the statistical power in genetic mapping was too low (Diaz. et.al. 2020). A strategy to increase the statistics were to increase the number of parents through recombination of inbred lines through multiple parents, or multi-parent advanced generation intercross (MAGIC) (Kover et al. 2009).

MAGIC is a mapping method where several founder lineages are intercrossed over multiple generations and eventually bred to create genetically diverse inbred lines. The MAGIC method creates genetically recombinant chromosomes from the founder haplotypes. Additionally, the MAGIC lines inherit alleles from all parents used in the crosses (Scott. et al. 2020). This results in a large allelic diversity and variation in phenotypes. The MAGIC lines of common bean used for this study were developed with inter-cross from eight Mesoamerican parental elite founder lines with different physiological traits and improved drought tolerance. The MAGIC population consist of 500 individual lines that were derived from the eight parental breeding lines through intercrosses. Four of the parent lines included interspecific introgression from runner bean (*P. coccineus*), year bean (*P. dumosus*) and tepary bean (*P. acutifolius*). A genetic map for the MAGIC lines had already been developed with a total length of 857 *cM* (Diaz. et al 2020). This genetic map was used for QTL-analysis to identify patterns of trait segregation within the lines.

2. Aim

The aim of this study was to investigate the genetic basis of variation in stomatal traits of common bean (*Phaseolus vulgaris*) using a MAGIC population, including the identification of associated loci, candidate genes and to what extent these traits share or differ in genetic regulation.

3. Material and method

3.1 Plant material and growth conditions

The beans were cultivated inside a climate chamber with the growth conditions set to 12 hours of daylight and 12 hours nighttime. During the daytime the temperature was set to 28°C, relative humidity (RH) was 40% and the light was set to ~450-550 $\mu mol \cdot m^{-2} \cdot s^{-1}$ at leaf level. During nighttime the settings where at 21°C, 80% RH. The beans were planted in separate pots (12x12x11 cm) a few centimeters deep into potting soil (Hasselfors garden, S-jord) that had been mixed with regular plant nutrition ("Stroller blå trädgårdsnäring") by the recommendations on the package. The plants spent three weeks inside to phytotron until some of their trifoliolate leaves were fully developed, during this period watering occurred twice a week.

In advance to the study epidermis peels had been prepared from 500 MAGIC lines of common bean and from the eight parent lineages. The epidermal peels were taken from fully grown leaves of the bean plants with fully developed stomata. The MAGIC lines were all numbered and the eight parent lines named as following: ALB213, INB827, INB841, MIB778, Sen56, SCR2, SCR9 and SXB412.

3.2 Investigation of stomatal traits

By attaching transparent adhesive scotch tape to the abaxial surface of a large, fully developed midleaf trifoliolate, the outermost epidermal layer was peeled onto the tape. The peels were taken from the lamina of the leaf to avoid any veins to ensure a high stomatal density as well as the same type of peel from each plant. From each plant two peels were taken, one from the left, and one from the right side of the leaf midrib. The epidermal peels were then transferred onto a microscope slide and marked with the line number.

Microscopy was carried out on epidermis peels from 200 bean plants of the MAGIC lines as well as 33 peels from the eight parental genotypes. The peels were studied through an Olympus BX60 microscope at 40x magnification with an attached campera. From each epidermal peel three photographs were taken at different locations. In cases when the left epidermal peel was insufficient for a clear photograph the right one was used instead. The stomata were mapped out on the photographs using the software WaveImage (version x64, 4.11.22004.20230115) by using the ellipsoid function in the software (figure 1). The ellipsoid provided data consisting of area and length of the stomata as well as width and diameter. The data also contained the number of ellipsoids which corresponded to the number of stomata per image. The data was transferred onto an excel sheet where the mean of stomatal area, length, width, and perimeter was calculated for each plant. The stomatal density was estimated by calculating the mean number of stomata per photograph from the three images, divided with the photographed total area of 90 035 μm^2. Furthermore, the maximal stomatal aperture was calculated using the formula $a_{max} = \pi(p/4)^2$ where p represents length of the stomata pore which was the same as stomatal length. Maximal conductance was also calculated according to the formula for g_{wmax}:

$$g_{wmax} = \frac{d}{v} * D * a_{max} / (l + \frac{\pi}{2}\sqrt{a_{max}/\pi})$$

Where d represent the diffusivity of water vapor which is constant at 25°C and has a value of $0.256 * 10^{-4}$, v is the molar volume of water vapor, and at 15°C it is 0.024465. D symbolize

stomatal density and a_{max} the calculated maximal aperture of stomata. Lastly l is the pore depth, and it is estimated to be the same as the guard cell width which is approximately half of the stomata width. The unit for maximal conductance is $mol\, m^{-2}s^{-1}$ and therefore all values that were measured in μm had to be transformed into m. (Franks & Beerling. 2009)

***Figure 1**. **Microscopic image of abaxial trifoliolate leaf epidermis of common bean.** Stomata are measured with a red outline using WaveImage, numbers represent length and width of adjacent stomata in micrometers. Scalebar = 10 µm.*

3.3 Data analysis

Data analysis was done in R (version 4.5.3) applying the packages dplyr, ggplot2, lme4, patchwork, performance and R/qtl2 (Broman. 2019) for data visualization, statistical modeling, and QTL mapping. Stomatal traits including area, density, length, and maximal conductance were analyzed for the eight parent lines and 200 MAGIC lines. Significant differences between parent lines were assessed using a one-way analysis of variance (ANOVA). Relationships between stomatal density and area were visualized using scatterplots and linear regression analysis for both parent- and MAGIC populations. When analyzing frequency distribution of traits in the 200 MAGIC lines values were natural log-transformed to improve the normality of the distribution. Lastly a QTL-analysis (quantitative traits locus) was performed were for the 200 MAGIC lines measured. Phenotypic data from the microscopy and genotypic data acquired from an earlier study were analyzed using a Haley-Knott regression to identify QTLs in the R/qtl2 package (Broman. 2019). The analysis identified genomic regions corresponding to trait differences. LOD thresholds with statistical significance were settled using 1000-permutation test. The results from the Haley-Knott scan were plotted into a graph, one for each stomatal trait, with a line that had peaks representing detected QTLs including a 1.5 confidence interval around the peak. Peaks that exceeded the LOD threshold represented significant peaks. LOD parameters were calculated from the peaks detected, that included in which chromosome the gene existed, at what centimorgan the peak was and its confidence interval as well as the LOD score for the peak.

Candidate genes located in the QTL regions were identified using the R package rtracklayer which was used to import genomic coordinates. Gene annotations for *Phaseolus vulgaris* were downloaded from Phytozome v.14 (Goodstein et al. 2012) using the P. vulgaris version 2.1 genome assembly. The QTL peak positions were converted from genetic positions (cM) to the physical positions (bp) to enable comparison with the genome annotation. Genes located within the peak region were extracted and ranked according to their physical distance from the QTL peak. Possible candidate genes were investigated using gene function annotations available in Phytozome. Genes with annotated functions potentially related to the stomatal trait associated with the QTL were identified as candidate genes.

4. Results

4.1 Genetic variation in common bean parental lines

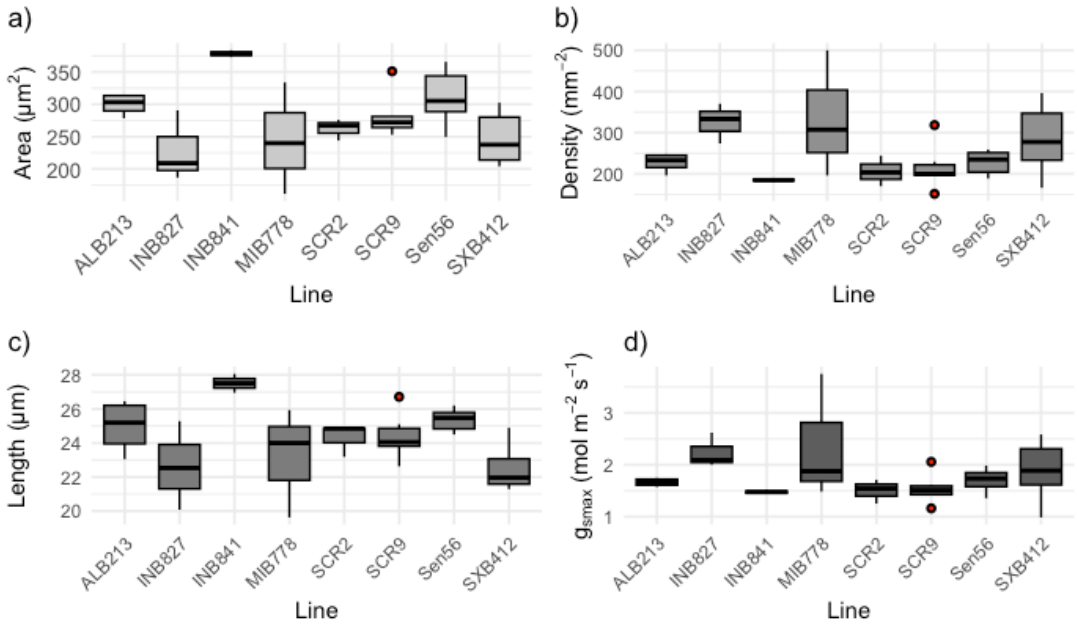

Figure 2. Distribution of stomatal traits across eight parental lines of common bean. *The parent lines: ALB213 (n=4), INB827 (n=3), INB841 (n=2), MIB778 (n=3), SCR2 (n=3), SCR9 (n=6), Sen56 (n=6) and SXB412 (n=6) are shown on the x-axis. The y-axis displays different morphological trait on the epidermis of midleaf trifoliolate of the bean plants. The traits are displayed as following: a) Stomatal area* (μm^2*; ANOVA, F = 3.49, p = 0.0095), b) Stomatal density* (mm^{-2}*; ANOVA, F = 2.25, p = 0.0640), c) Length per stomata (µm; ANOVA, F = 3.26, p = 0.0134) and d) Maximal stomatal conductance,* g_{smax} ($mol\ m^{-2}s^{-1}$*; ANOVA, F = 1.62, p = 0.1754). The boxes represent the upper and lower quartile as well as the median shown as a black line inside the box. Outliers are shown as solid red dots either above or below the boxes.*

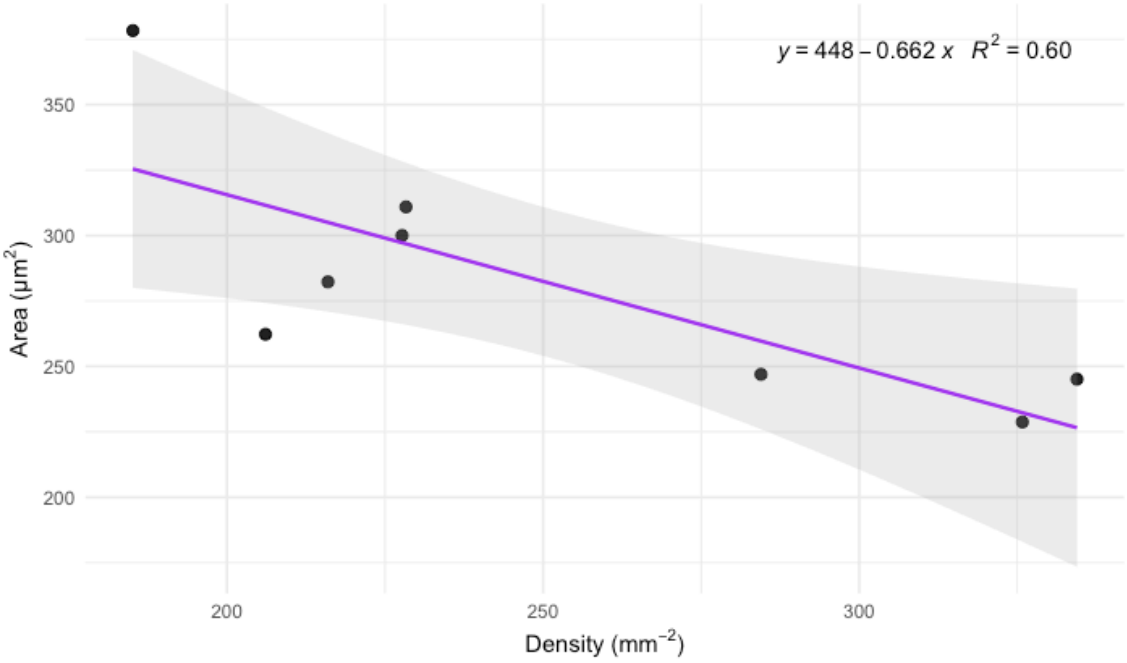

Figure 3. Relationship between stomatal area and density in parental lines of common bean. *Stomatal density* ($stomata/mm^2$) *is shown on the x-axis and area* (μm^2) *on the y-axis. Each dot represents the average for one of the eight parent lines. The fitted regression line (y = 448-0.0662x,* $R^2 = 0.60$*) indicates the relationship between stomatal density and area with a shaded 95% confidence interval.*

There is variation in morphological traits across the different parent lines of common bean (figure 2). Most of the lines share a similar median for stomatal area around 250 μm^2, the exception is for INB841 with an average area of ~380 μm^2. INB827 and SXB412 have lower medians than the rest of the parent lines (~230-245). For density MIB778 and INB827 have the largest number of stomata (~330 mm^{-2}) and INB841 have the lowest median density (~185 mm^{-2}). The remaining five lines show overlapping densities at around 210-280 mm^{-2}. The medians for length show a similar result as the medians for stomatal area with INB841 having the longest stomata (~27.5 µm) and SXB412 at the bottom (~22 µm). However, the differences in largest and smallest stomatal length are not as large. For maximal conductance (g_{smax}) the median variation is smaller. All lines have a median around 2.0 $mol\, m^{-2} s^{-1}$. For all four morphological traits, MIB778 displayed the largest interquartile range which is a result of greater variance within the sample of that parent line. SCR9 have upper or under outliers for all traits which indicate that at least one sample within the line show unusually large stomata or density than the rest of the sample. Furthermore, the ANOVA analysis indicate that there are significant differences connected to the parent lineage for area and length ($p < 0.05$). Stomatal density ($p = 0.0640$) and maximal conductance ($p = 0.1754$) did not show statically significant differences.

There is evidence of a negative linear relationship between stomatal density and area among the eight parent lines (figure 3) which indicate that as stomatal area increases, density decreases. Additionally, there is a relatively large 95% confidence interval surrounding the fitted line. The regression lines $R^2 = 0.60$ demonstrate that 60% of the variation of stomatal area can be explained by stomatal density. It can be concluded that parent lines with larger stomata tended to have a lower density and the other way around for other lines.

4.2 Genetic mapping of common bean MAGIC lines

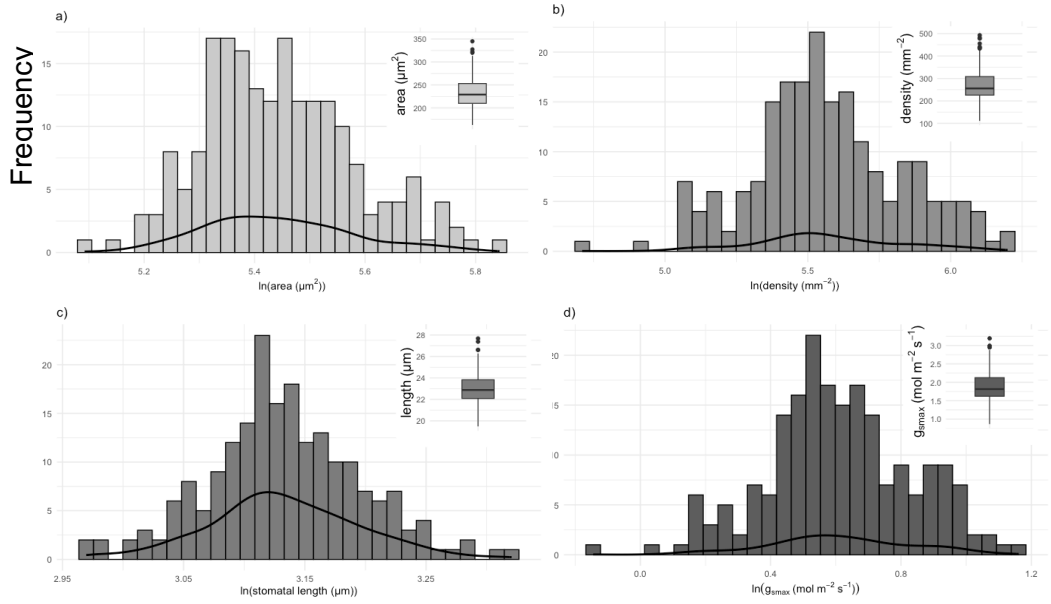

Figure 4. Frequency distribution of different stomatal traits in MAGIC lines of common bean*. The histograms correspond to a) natural logarithm (ln) of stomatal area (μm^2), b) ln(stomatal density (mm^{-2})), c) ln(stomatal length (µm)) and d) ln(g_{smax} ($mol\, m^{-2} s^{-1}$), representing the maximal conductance of stomata). The x-axis represents the natural log-transformed trait values and the y-axis show frequency of observations across the sample. Inset boxplots represent median, interquartile range and outliers for each trait.*

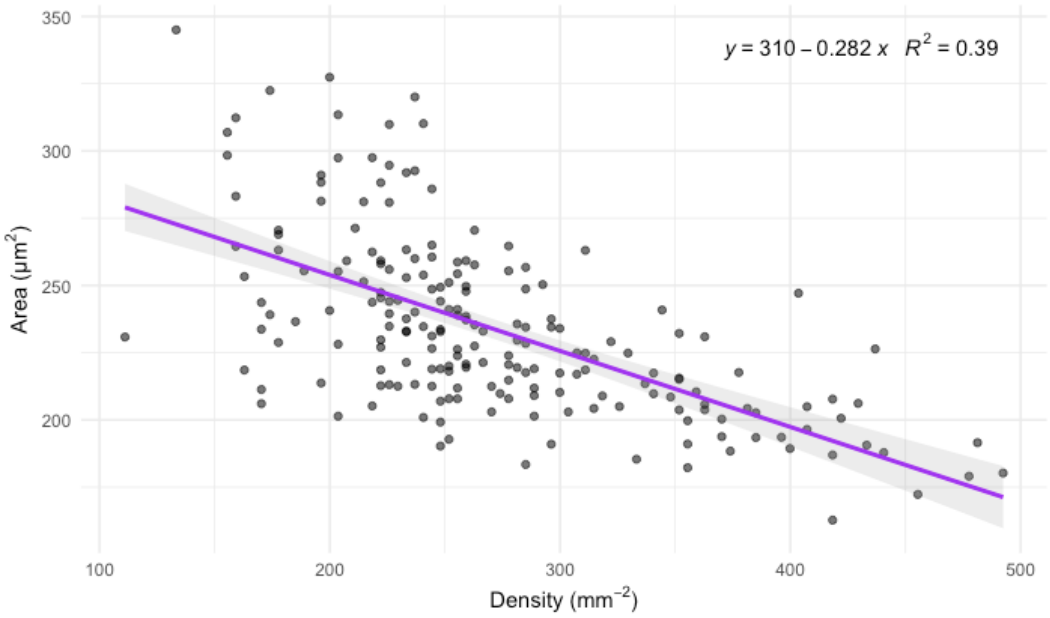

Figure 5. Relationship between stomatal density and stomatal area in MAGIC lines of common bean. *Stomatal density* $(stomata/mm^2)$ *is shown on the x-axis and area* (μm^2) *on the y-axis. The fitted regression line (y = 310-0.0282x* R^2 *= 0.39) indicates the relationship between stomatal density and area with a shaded 95% confidence interval. Each point represents one single MAGIC line.*

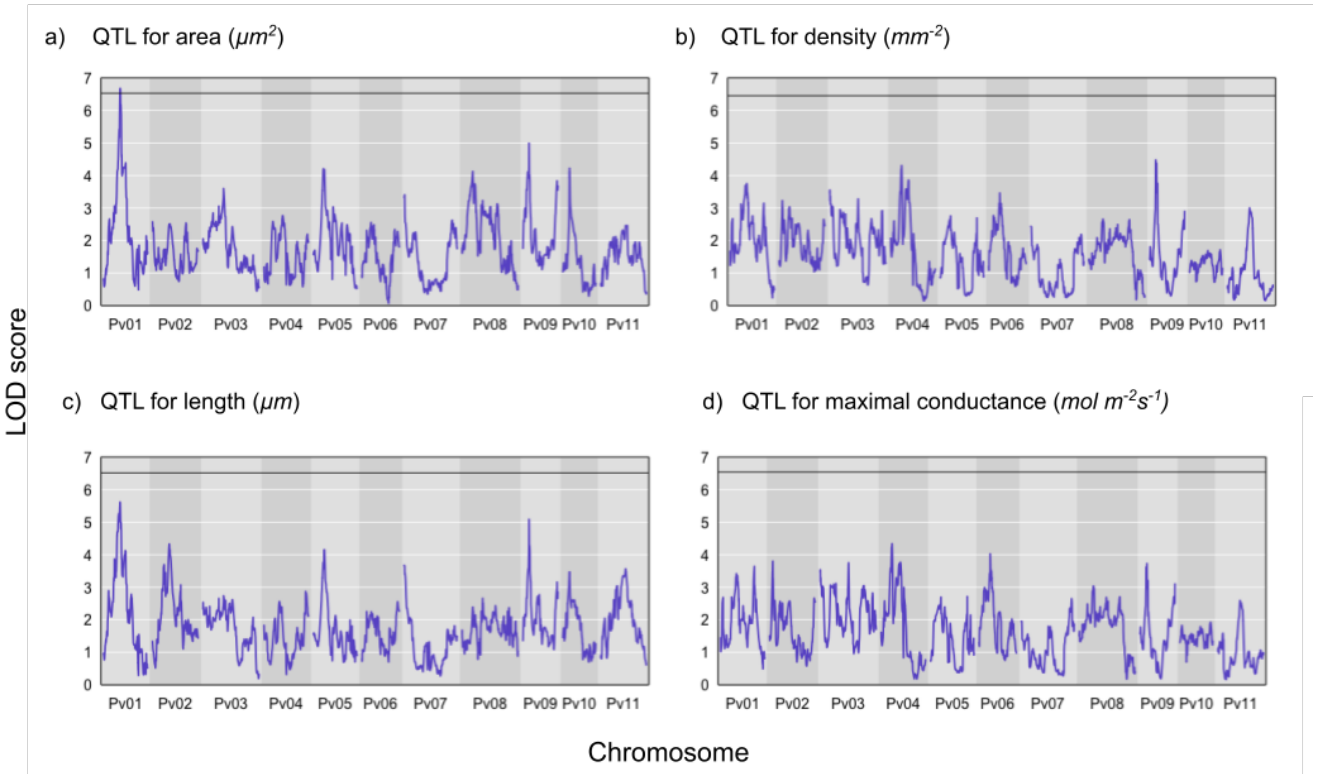

Figure 6. QTL-mapping over different stomatal traits among MAGIC lines of common bean. *Chromosomes (Pv01-Pv11) of Phaseolus vulgaris are shown on the x-axis and LOD scores on the y-axis. The black horizontal lines indicate significant thresholds for each trait. a) Stomatal area (LOD threshold: 6.53): one QTL-score exceed the significance threshold; peak summary: Chr: Pv01, peak: 29.07 cM, LOD-score: 6.677, confidence interval (CI): 26.62-31.36 cM. b) Stomatal density (LOD threshold: 6.45): no significant QTL. c) Stomatal length (LOD threshold: 6.52): no significant QTL. d) Maximal conductance (LOD threshold: 6.54): no significant QTL.*

Microscopic examination of epidermal prints from 200 MAGIC lines revealed clear variation in stomatal morphology. Stomata were successfully identified and measured using image analysis software (figure 1). The stomata were distributed irregularly across the epidermis surface with varying size and density observed among the lines.

The frequency distributions for the natural log-transformed epidermal morphological traits measured in the midleaf trifoliolate of common bean MAGIC lines where generally normal (figure 4). The distribution for ln(area) (figure 4a) was slightly left skewed with two peaks, however it is not bimodal, and most observations were centered around 5.4 μm^2. Furthermore ln(density) (figure 4b), ln(length) (figure 4c) and ln(g_{smax}) (figure 4d) all had unimodal distribution with one peak in the middle and some variation without any extreme outliers. However, ln(length) has a slightly tighter spread and smaller variation than the other three stomatal traits.

The correlation between stomatal density and area in MAGIC lines of common bean resulted in a negative relationship similarly to the parent lines revealed by the function equation y = 310 – 0.282x (figure 4). R^2= 0.39 reveal that there is a 39% certainty that the variation of stomatal area is depending on density. There is a larger spread of stomatal area among MAGIC lines within lower density half of the graph and the range gets smaller following the regression line as density gets higher. The 95% confidence interval is tightly surrounding the fitted regression line.

QTL-mapping of the four common bean traits resulted in one QTL peak for stomatal area (figure 6). The QTL peak is at chromosome 1 (Pv01) at 29.7 *cM* with the LOD score 6.677 and a confidence interval ranging from 26.62-31.36 *cM* (figure 6a). The QTL for density (figure 6b) and g_{smax} (figure 6d) show similar trends in LOD scores although no QTLs reach the threshold and are significant. Neither the QTL for length (figure 6c) show any significant QTLs. However, the peaks are similar to the ones in area suggesting both stomatal traits may be controlled by the same genes. The QTL-peak associated with stomatal area identified 95 possible candidate genes within the 1.5-LOD confidence interval surrounding the peak (Appendix, Table 1). The distance between the candidate genes and the peak ranged from approximately 5030-957200 bp. There is no immediate candidate that stands out when it comes to gene function, however some correlation can be detected. Most of the genes are some types of kinesins or code for a signaling protein. Multiple genes are missing information, and it is therefore unknown if they play an important role in determining stomatal area. In some parts of the list multiple genes have the exact same function which may be the case in common bean or a mistake.

5. Discussion

Trait variation could be observed in the eight parental lines of common bean, indicating genetic diversity of stomatal traits (figure 2). Among the measured traits, stomatal area displayed a significant variation between lines (ANOVA; p = 0.0095) while stomatal density, length and maximal conductance exhibited differences that were not significant. An important note is that, when measured stomata dimensions can vary depending on the time of sampling and at what rate the stomata are opened or closed. However, it is unlikely that the opening status would affect measured stomatal area. This is because area reflect the size of the entire guard cell complex and if the stomata are open, guard cells swell and increase in width but also decrease in length. The change does not affect the total area since it is calculated based on both length and width. Therefore, observed differences in stomatal area where most likely due to underlying genetic variation and not physiological changes in stomatal aperture.

Maximal conductance (g_{wmax}) was less variable among parent lines, with a stable median. This may be because g_{wmax} is calculated based on both stomatal density and length. Since the calculation is based on both traits with opposing changes that cancel each other out variation in these traits are neutralized. Furthermore, it is biologically plausible that there is less variation in the plants total gas exchange to obtain physiological optimization while stomatal length and density

on the other hand are more variable traits during development (Lawson & Blatt. 2014). A noticeable exception of variation is MIB778 with a much wider interquartile range in comparison to the other lines. The broad variation could be due to inconsistent sampling locations on the bean leaf, as stomatal density varies between the basal, median, and apical regions of the leaf. However, epidermal prints were attempted to be obtained from similar regions of all bean plants to avoid this error. Another explanation could be that the line itself has a large within line variability resulting in a large spread and intraspecific variation, but more replicates were needed to conclude this. There was an attempt to grow more replicates of parent lines. However, only four lines germinated properly (ALB213, SCR2, SCR9, Sen56 and SXB412) and could be used as epidermal peels for microscopy. In addition, it is possible that the increased variation is related to the lines genetic background. MIB778 contained introgression from year bean (*Phaseolus* dumosus), which could contribute with allelic variation that is not present in the other parent lines. However, investigation of the allelic attributes of the introgression region would be required to evaluate this.

There is evidence of a correlation between stomatal area and density among the parent and MAGIC population indicating that large stomata are related to a lower density and vice versa (figure 3; figure 5) This relationship was to be expected since the leaf epidermal has a maximum amount of space for stomata (Harrison et al. 2019). The strength of relationships differs between the parent and MAGIC population. The parent lines correlations relatively wide confidence interval indicates uncertainty likely due to the few datapoint being parent line means instead of all replicates (figure 5). Although 60% of the variation in density can be explained by stomatal area which strengthens the relationship. Datapoint of the MAGIC lines mostly display a wide variation in stomatal area at lower densities indicating that this negative relationship is not always as expected. When the stomatal density is lower it allows for a broader flexibility in stomatal size in comparison to when density is higher because of the physical constraint of cell space on the epidermis. The MAGIC population exhibited greater variation for the other stomatal traits as well in comparison to parent line, likely due to both biological and statistical reasons. The MAGIC population are expected to exhibit more allelic diversity and increased recombination in comparison to the parent lines with more fixed genotypes (Diaz et al. 2020), which can profess the wider range of variance. In addition, the MAGIC population consisted of a larger sample size (200 individuals) in comparison to the parent population of 33 replicates among the eight lines. It is likely that the larger sample size provided a more extensive representation of the trait distribution with included extreme values that might be missed in smaller datasets. The few amounts of replicates per parent lines may also have failed to represent true within line variation.

The QTL-analysis found a significant QTL for stomatal area at Pv01 which suggest there is a genetic factor regulating stomatal development in this region. There was also an encountered QTL-peak at chromosome 1 for stomatal perimeter, which was tested during trial. Although, the peak was nearly identical to the one detected for stomatal area and therefore we decided to only include one of the two traits in the results. Perimeter and area are likely closely related traits, as both reflect stomatal size, and therefore may be influenced by shared genetic mechanisms controlling stomatal development (Bertolino et al. 2019). No significant QTL-peaks were found for the other stomatal traits and this is likely due to insufficient number of lines. If we were to include all 500 MAGIC lines available there might have been a different outcome in the QTL analysis. However, the missing peaks may indicate that stomatal area is regulated independently from stomatal density. The QTL-peak for area included 95 possible candidate genes within the 1.5 LOD support interval (Appendix 1, Table 1). Genes closer to the peak are generally more likely in linkage with the gene that influence the trait. However, physical proximity is not the main factor that should decide candidate gene prioritization. Candidate genes potentially associated with the regulation of stomatal area include leucine rich repeats (LRRs), receptor-like kinases (RLKs), MYB transcription factors and AP2/ERF transcription factors, which all have established roles in stomatal development and in *Arabidopsis thaliana* (Zhou et.al. 2026). Among the genes within the QTL interval, the candidate gene closest to the peak is an LLR-RLK. In Arabidopsis

these genes are involved in stomatal initiation and patterning making these reasonable candidates for further investigation. However, functional information from Arabidopsis may not adapt to common bean and therefore these genes should be considered candidates and not confirmed as regulator of stomatal area, further investigation and functional validation is needed. Furthermore, several genes within the QTL interval lack functional annotations with unknown functions in Phytozome. Due to limited information their potential role in stomatal area regulation cannot be concluded.

6. Conclusion

The parent genotypes showed consistent relationships of stomatal traits between lines. It could be ascertained that the stomata were generally either few and large or more tightly packed and smaller in size, which demonstrate the expected tradeoff between stomatal size and density. Stomatal area exhibited significant variation among parent lines compared to the other investigated traits, suggesting that there are genetic differences influencing stomatal size within the population. The relatively stable variation in maximal conductance (g_{wmax}) suggest a compensatory relationship between stomatal density and size which may contribute to maintaining physiological optimization in gas exchange.

A clear negative correlation between stomatal density and stomatal area was observed in both parent and MAGIC populations supporting the concept that physical constraint within the leaf epidermis limit the occurrence of both large and tightly packed stomata. However, the MAGIC population revealed that lower stomatal densities allow greater flexibility in stomatal size, which indicate that this negative relationship is not absolute. The greater phenotypic variation observed in the MAGIC population is likely explained by increased allelic diversity, recombination, and a larger sample size in comparison to the parent lines.

The QTL-analysis identified a significant locus for stomatal area on chromosome 1 which suggest the presence of genetic factors involved in stomatal size regulation and development in this region. No significant QTLs were detected for the remaining stomatal traits, which may reflect limited statistical power due to a relatively small number of MAGIC lines analyzed. 95 candidate genes were identified within the QTL interval including leucine rich repeats (LLRs) and receptor like kinases (RLKs) which are associated with stomatal development in other plant species and therefore represent a promising target for future investigation of trait regulation in common bean. To determine their role in regulating stomatal area, further functional validation would be required. Overall, these findings provide valuable insight into the genetic and phenotypic regulation of stomatal traits in common bean and establish a foundation for continued studies investigating genetic mechanisms underlying stomatal development and physiological adaption.

Acknowledgements

I want to thank my supervisor for this project, Mats Andersson for all the feedback regarding my thesis writing and for answering any questions about the project. I also want to give a big thank you to Diana Laura Labastida James for providing me with the prepared epidermal peels from the MAGIC and parent population as well as for handing me a prewritten R-script for genetic mapping and sorting out any confusion regarding the programming and questions overall.

7. References

Bertolino, L. T., Caine, R. S., & Gray, J. E. (2019). Impact of Stomatal Density and Morphology on Water-Use Efficiency in a Changing World. *Frontiers in Plant Science*, *10*, 225. https://doi.org/10.3389/fpls.2019.00225

Bitocchi, E., Rau, D., Bellucci, E., Rodriguez, M., Murgia, M. L., Gioia, T., Santo, D., Nanni, L., Attene, G., & Papa, R. (2017). Beans (Phaseolus ssp.) as a Model for Understanding Crop Evolution. *Frontiers in Plant Science*, *8*, 722. https://doi.org/10.3389/fpls.2017.00722

Broman, K. W., Gatti, D. M., Simecek, P., Furlotte, N. A., Prins, P., Sen, Ś., Yandell, B. S., & Churchill, G. A. (2019). R/qtl2: Software for Mapping Quantitative Trait Loci with High-Dimensional Data and Multiparent Populations. *Genetics*, *211*(2), 495–502. https://doi.org/10.1534/genetics.118.301595

Castro-Guerrero, N. A., Isidra-Arellano, M. C., Mendoza-Cozatl, D. G., & Valdés-López, O. (2016). Common Bean: A Legume Model on the Rise for Unraveling Responses and Adaptations to Iron, Zinc, and Phosphate Deficiencies. *Frontiers in Plant Science*, *7*. https://doi.org/10.3389/fpls.2016.00600

Clark, D. P., & Pazdernik, N. J. (2016). Genomics and Gene Expression. In *Biotechnology* (pp. 249–294). Elsevier. https://doi.org/10.1016/B978-0-12-385015-7.00008-9

Des Roches, S., Post, D. M., Turley, N. E., Bailey, J. K., Hendry, A. P., Kinnison, M. T., Schweitzer, J. A., & Palkovacs, E. P. (2017). The ecological importance of intraspecific variation. *Nature Ecology & Evolution*, *2*(1), 57–64. https://doi.org/10.1038/s41559-017-0402-5

Diaz, S., Ariza-Suarez, D., Izquierdo, P., Lobaton, J. D., De La Hoz, J. F., Acevedo, F., Duitama, J., Guerrero, A. F., Cajiao, C., Mayor, V., Beebe, S. E., & Raatz, B. (2020). Genetic mapping for agronomic traits in a MAGIC population of common bean (Phaseolus vulgaris L.) under drought conditions. *BMC Genomics*, *21*(1), 799. https://doi.org/10.1186/s12864-020-07213-6

Goodstein, D. M., Shu, S., Howson, R., Neupane, R., Hayes, R. D., Fazo, J., Mitros, T., Dirks, W., Hellsten, U., Putnam, N., & Rokhsar, D. S. (2012). Phytozome: A comparative platform for green plant genomics. *Nucleic Acids Research*, *40*(D1), D1178–D1186. https://doi.org/10.1093/nar/gkr944

Harrison, E. L., Arce Cubas, L., Gray, J. E., & Hepworth, C. (2020). The influence of stomatal morphology and distribution on photosynthetic gas exchange. *The Plant Journal*, *101*(4), 768–779. https://doi.org/10.1111/tpj.14560

Haworth, M., Marino, G., Materassi, A., Raschi, A., Scutt, C. P., & Centritto, M. (2023). The functional significance of the stomatal size to density relationship: Interaction with atmospheric [CO2] and role in plant physiological behaviour. *Science of The Total Environment*, *863*, 160908. https://doi.org/10.1016/j.scitotenv.2022.160908

Hetherington, A. M., & Woodward, F. I. (2003). The role of stomata in sensing and driving environmental change. *Nature*, *424*(6951), 901–908. https://doi.org/10.1038/nature01843

Hummel, M., Hallahan, B. F., Brychkova, G., Ramirez-Villegas, J., Guwela, V., Chataika, B., Curley, E., McKeown, P. C., Morrison, L., Talsma, E. F., Beebe, S., Jarvis, A., Chirwa, R., & Spillane, C. (2018). Reduction in nutritional quality and growing area suitability of common bean under climate change induced drought stress in Africa. *Scientific Reports*, *8*(1), 16187. https://doi.org/10.1038/s41598-018-33952-4

Kover, P. X., Valdar, W., Trakalo, J., Scarcelli, N., Ehrenreich, I. M., Purugganan, M. D., Durrant, C., & Mott, R. (2009). A Multiparent Advanced Generation Inter-Cross to Fine-Map Quantitative Traits in Arabidopsis thaliana. *PLoS Genetics*, *5*(7), e1000551. https://doi.org/10.1371/journal.pgen.1000551

Lawson, T., & Blatt, M. R. (2014). Stomatal Size, Speed, and Responsiveness Impact on Photosynthesis and Water Use Efficiency. *Plant Physiology*, *164*(4), 1556–1570. https://doi.org/10.1104/pp.114.237107

Pathania, A., Sharma, S. K., & Sharma, P. N. (2014). Common Bean. In M. Singh, I. S. Bisht, & M. Dutta (Eds.), *Broadening the Genetic Base of Grain Legumes* (pp. 11–50). Springer India. https://doi.org/10.1007/978-81-322-2023-7_2

Polania, J. A., Poschenrieder, C., Beebe, S., & Rao, I. M. (2016). Effective Use of Water and Increased Dry Matter Partitioned to Grain Contribute to Yield of Common Bean Improved for Drought Resistance. *Frontiers in Plant Science*, *7*. https://doi.org/10.3389/fpls.2016.00660

Samantara, K., Shiv, A., De Sousa, L. L., Sandhu, K. S., Priyadarshini, P., & Mohapatra, S. R. (2021). A comprehensive review on epigenetic mechanisms and application of epigenetic modifications for crop improvement. *Environmental and Experimental Botany*, *188*, 104479. https://doi.org/10.1016/j.envexpbot.2021.104479

Scott, M. F., Ladejobi, O., Amer, S., Bentley, A. R., Biernaskie, J., Boden, S. A., Clark, M., Dell'Acqua, M., Dixon, L. E., Filippi, C. V., Fradgley, N., Gardner, K. A., Mackay, I. J., O'Sullivan, D., Percival-Alwyn, L., Roorkiwal, M., Singh, R. K., Thudi, M., Varshney, R. K., … Mott, R. (2020). Multi-parent populations in crops: A toolbox integrating genomics and genetic mapping with breeding. *Heredity*, *125*(6), 396–416. https://doi.org/10.1038/s41437-020-0336-6

Seidl, F., Linder, R., & Ehrenreich, I. M. (2016). Quantitative Trait Variation, Molecular Basis of. In *Encyclopedia of Evolutionary Biology* (pp. 388–394). Elsevier. https://doi.org/10.1016/B978-0-12-800049-6.00059-7

Yoosefzadeh-Najafabadi, M., D.Singh, K., Pourreza, A., S.Sandhu, K., Adak, A., C.Murray, S., Eskandari, M., & Rajcan, I. (2023). Remote and proximal sensing: How far has it come to help plant breeders? In *Advances in Agronomy* (Vol. 181, pp. 279–315). Elsevier. https://doi.org/10.1016/bs.agron.2023.05.004

Zhou, W., Wang, W., Zhao, M., Li, Y., He, H., & Zhou, Y. (2026). Regulation of stomatal development by receptor-like kinases and receptor-like proteins in Arabidopsis and grasses. *Frontiers in Plant Science*, *17*, 1770946. https://doi.org/10.3389/fpls.2026.1770946

Appendix 1

Table 1. List of candidate genes within the 1.5 LOD support interval of the QTL-peak for stomatal area. *Gene annotations and functional description from PhytozomeV14.*

Gene ID	*Chr*	*Strand*	*Position (bp)*	*Distance to QTL-peak (bp)*	*Domain*	*Predicted function*
Phvul.001G038400	Chr01	+	4638226-4647093	5028,667	Leucine-rich repeat (LRR)	Ribonuclease Inhibitor
Phvul.001G038500	Chr01	-	4624156-4624745	8452,333	unknown	unknown
Phvul.001G038600	Chr01	-	4622622-4624035	9162,333	unknown	unknown
Phvul.001G038700	Chr01	+	4610309-4621135	12062,333	F-box	Ribonuclease Inhibtor
Phvul.001G038850	Chr01	+	4651885-4658991	18687,667	P-loop NTP hydrolase	Kinesin
Phvul.001G039301	Chr01	+	4659457-4666077	26259,667	P-loop NTP hydrolase	Kinesin
Phvul.001G038800	Chr01	+	4588596-4593058	40139,333	FAD-binding protein	UDP-N-acetylglucosamine enzyme
Phvul.001G045700	Chr01	-	4677486-4682150	44288,667	Aldehyde dehydrogenase	Aldehyde Dehydrogenase
Phvul.001G045800	Chr01	-	4684845-4685288	51647,667	unknown	unknown
Phvul.001G045900	Chr01	-	4700948-4704329	67750,667	Armadillo repeat	Leucine-rich repeat protein
Phvul.001G038900	Chr01	+	4559337-4560801	72396,333	PHF5-like protein	Pre-mRNA-splicing factor
Phvul.001G039000	Chr01	-	4552734-4557258	75939,333	Zinc finger (RING-type)	Zinc finger (RING-type)
Phvul.001G046100	Chr01	+	4750369-4762562	117171,667	Helicase (UvrB-like)	Tandem AAA-ATPase
Phvul.001G039100	Chr01	-	4510889-4515611	117586,333	Methyltransferase (SAM-dependent)	Viral methyltransferase (VP39-like)
Phvul.001G039200	Chr01	+	4509901-4510542	122655,333	Photosystem II (PsbX)	Helical protein
Phvul.001G039300	Chr01	+	4499497-4508975	124222,333	Protein kinase	Phosphorylase kinase
Phvul.001G039400	Chr01	+	4490927-4492051	141146,333	unkown	unknown
Phvul.001G046200	Chr01	+	4781922-4788523	148724,667	Chloramphenicol acetyltransferase	Chloramphenicol acetyltransferase
Phvul.001G046300	Chr01	-	4793935-4798437	160737,667	MYB transcription factor	Rossmann-fold enzyme
Phvul.001G046400	Chr01	-	4817633-4819959	184435,667	Chitinase-related	Chitinase
Phvul.001G039500	Chr01	-	4440541-4444766	188431,333	Alfin-like protein	Zinc finger (RING-type)
Phvul.001G039600	Chr01	+	4425303-4429029	204168,333	Mitochondrial carrier	Mitochondrial carrier
Phvul.001G046500	Chr01	+	4838124-4838990	204926,667	Zinc finger (C2H2)	Zink finger protein
Phvul.001G039700	Chr01	-	4422500-4423347	209850,333	HSP20 chaperone	Immunoglobulin-like protein
Phvul.001G039800	Chr01	-	4420208-4421138	212059,333	HSP20 chaperone	Immunoglobulin-like protein
Phvul.001G046600	Chr01	-	4851741-4853736	218543,667	Mitochondrial glycoprotein	Mitochondrial matrix protein
Phvul.001G039900	Chr01	-	4409993-4411458	221739,333	WRKY domain	WRKY transcription factor
Phvul.001G046700	Chr01	+	4862126-4864641	228928,667	PPPDE peptidase	PPPDE peptidase
Phvul.001G040000	Chr01	-	4399520-4401949	231248,333	Lectin/glucanase	Transferase (phosphotransferase)
Phvul.001G040100	Chr01	-	4394207-4396266	236931,333	Protein kinase	Jelly roll fold protein
Phvul.001G046800	Chr01	-	4872187-4874180	238989,667	DUF868 protein	unknown
Phvul.001G040750	Chr01	+	4388488-4392444	240753,333	EEIG1/EHBP1-like	unknown
Phvul.001G040300	Chr01	+	4379952-4382583	250614,333	Tyrosine kinase	Jelly roll fold protein
Phvul.001G040400	Chr01	+	4370066-4372118	261079,333	Tyrosine kinase	Transferase (phosphotransferase)
Phvul.001G040500	Chr01	+	4359201-4361618	271579,333	Tyrosine kinase	Transferase (phosphotransferase)
Phvul.001G046900	Chr01	-	4924736-4926129	291538,667	AP2/ERF transcription factor	AP2/ERF transcription factor
Phvul.001G040600	Chr01	-	4339156-4340979	292218,333	Protein kinase	Phosphorylase kinase
Phvul.001G040700	Chr01	+	4336106-4338606	294591,333	Protein kinase	Phosphorylase kinase
Phvul.001G040800	Chr01	-	4327634-4329496	303701,333	Lectin/glucanase	Jelly roll fold protein
Phvul.001G040900	Chr01	+	4318144-4324991	308206,333	Enhancer of rudimentary	Enhancer of rudimentary protein
Phvul.001G047001	Chr01	+	4950443-4955184	317245,667	Aminotransderase	Aspartate aminotransferase
Phvul.001G041000	Chr01	+	4311086-4313782	319415,333	MFS transporter	MFS general substrate transporter
Phvul.001G047100	Chr01	-	4955650-4961025	322452,667	Protein kinase	Phosphorylase kinase
Phvul.001G041100	Chr01	+	4301662-4307479	325718,333	Antioxidant enzyme (AhpC-like)	Glutaredoxin
Phvul.001G047200	Chr01	-	4966056-4972213	332858,667	YAP-binding / ALF4-like	Glomulin-like protein
Phvul.001G041200	Chr01	-	4288230-4295546	337651,333	PPM phosphatase	PP2C phosphatase
Phvul.001G047300	Chr01	+	4972376-4981168	339178,667	TRAPP II complex protein	TRAPP complex protein
Phvul.001G047400	Chr01	-	4985485-4986274	352287,667	unknown	unknown
Phvul.001G041300	Chr01	-	4274941-4279243	353954,333	unknown	unknown
Phvul.001G041400	Chr01	+	4273585-4274937	358260,333	Phytocyanin	Cupredoxins (blue copper proteins)
Phvul.001G047500	Chr01	+	4995091-4995636	361893,667	Ribosomal protein (uS11)	Ribosomal protein S11
Phvul.001G041500	Chr01	-	4270729-4271258	361939,333	unknown	unknown
Phvul.001G041600	Chr01	+	4264578-4269382	363815,333	MFS transporter	Transmembrane protein
Phvul.001G047600	Chr01	+	4998189-5001247	364991,667	unknown	HPAT
Phvul.001G047700	Chr01	-	5001310-5019579	368112,667	Extended PHD domain protein	Zink finger protein
Phvul.001G041700	Chr01	-	4239451-4244391	388806,333	BTB/POZ protein	Potassium channel
Phvul.001G041800	Chr01	-	4227182-4238471	394726,333	Crotonase	Enoyl-CoA hydratase
Phvul.001G041900	Chr01	+	4222305-4225713	407484,333	Chorismate mutase	Chorismate mutase
Phvul.001G042000	Chr01	-	4175137-4198384	434813,333	C2 domain protein	Formin protein
Phvul.001G042100	Chr01	+	4172646-4174531	458666,333	WRKY domain	WRKY transcription factor
Phvul.001G042200	Chr01	+	4158732-4160336	472861,333	WRKY domain	WRKY transcription factor
Phvul.001G042300	Chr01	-	4125105-4139019	494178,333	TFIID subunit (TAF5)	Quinoprotein dehydrogenase-like
Phvul.001G042400	Chr01	+	4081421-4085877	547320,333	ER membrane complex protein	Transmembrane protein 85
Phvul.001G042500	Chr01	+	4074708-4079298	553899,333	Membrane protein	EamA-like transporter
Phvul.001G042600	Chr01	+	4065731-4071763	561434,333	Glycosyltransferase family 28)	Glycogen phosphorylase
Phvul.001G042700	Chr01	+	4059247-4063057	570140,333	Ska2-like protien	Coiled-coil protien
Phvul.001G042800	Chr01	+	4050181-4052709	580488,333	Leucine-rich repeat (LRR)	Ribonuclease Inhibitor
Phvul.001G043450	Chr01	+	4036528-4039925	593272,333	Leucine-rich repeat (LRR)	Ribonuclease Inhibitor
Phvul.001G043901	Chr01	+	4038640-4039167	594030,333	Leucine-rich repeat (LRR)	Ribonuclease Inhibitor
Phvul.001G043000	Chr01	+	4030665-4033321	599876,333	Leucine-rich repeat (LRR)	Ribonuclease Inhibitor
Phvul.001G043100	Chr01	-	4016061-4018434	614763,333	Ascorbate peroxidase	Peroxidase
Phvul.001G043200	Chr01	+	4010968-4013393	619804,333	DUF1336 protein	unknown
Phvul.001G043300	Chr01	+	4005758-4006531	626666,333	unknown	Expressed protein
Phvul.001G043400	Chr01	-	3986503-3991888	641309,333	PPM-type phosphatase	Phosphatase
Phvul.001G043500	Chr01	+	3977339-3978103	655094,333	unknown	Glutamine dumper protein
Phvul.001G043600	Chr01	+	3949356-3957315	675882,333	Histidine kinase	PAS domain protein
Phvul.001G043700	Chr01	-	3924909-3931637	701560,333	Papain-like cycsteine peptidase	Cysteine protease
Phvul.001G043800	Chr01	-	3921305-3924197	709000,333	Kelch repeat protein	Monooxygenase
Phvul.001G043900	Chr01	-	3910690-3914039	719158,333	Zinc finger (Ring/FYVE/PHD-type)	Zinc finger (RING-type)
Phvul.001G044000	Chr01	+	3905756-3909533	723664,333	Dioxygenase (2-oxoglutarate-dependent)	Dioxygenase (clavaminate-like)
Phvul.001G044100	Chr01	-	3893967-3900161	733036,333	Alpha/beta hydrolase	Alpha/beta hydrolase
Phvul.001G044200	Chr01	-	3863348-3864531	768666,333	unknown	unknown
Phvul.001G044300	Chr01	-	3847968-3848579	784618,333	unknown	unknown
Phvul.001G044400	Chr01	-	3835436-3836623	796574,333	unknown	unknown
Phvul.001G044500	Chr01	-	3805613-3806302	826895,333	unknown	unknown
Phvul.001G044600	Chr01	+	3793240-3798234	834963,333	SMR domain protien	Ribosomal protein S8
Phvul.001G044700	Chr01	-	3764312-3765606	867591,333	DUF1677 protein	DUF1677 protein
Phvul.001G044800	Chr01	+	3740734-3749689	883508,333	7-transmembrane domain (GPCR)	G protein-coupled receptor (GCR1)
Phvul.001G044900	Chr01	+	3734007-3738171	895026,333	Tyrosine kinase	Protein kinase
Phvul.001G045000	Chr01	+	3725590-3726360	906837,333	unknown	unknown
Phvul.001G045100	Chr01	+	3720002-3724520	908677,333	UspA-like / protein kinase	Ubiquitin-related transferase
Phvul.001G045200	Chr01	-	3705173-3714386	918811,333	Cyclophilin	Cyclophilin
Phvul.001G045300	Chr01	-	3683856-3688739	944458,333	PPM-type phosphatase	PP2C phosphatase
Phvul.001G045400	Chr01	-	3677580-3680026	953171,333	UspA kinase-lika	Jelly roll fold protein
Phvul.001G045500	Chr01	+	3671182-3675981	957216,333	General transporter (MFS-like)	MFS transporter